

Kernel Method based on Non-Linear Coherent State

Prayag Tiwari ^{1,*}, Shahram Dehdashti ^{2,†}, Abdul Karim Obeid ², Massimo Melucci ¹, and Peter Bruza ^{2‡}

¹ *Department of Information Engineering, University of Padova, Padova, 35131, Italy. and*

² *School of Information Systems, Queensland University of Technology, Brisbane 4000, Australia.*[§]

(Dated: July 17, 2020)

In this paper, by mapping datasets to a set of non-linear coherent states, the process of encoding inputs in quantum states as a non-linear feature map is re-interpreted. As a result of this fact that the Radial Basis Function is recovered when data is mapped to a complex Hilbert state represented by coherent states, non-linear coherent states can be considered as natural generalisation of associated kernels. By considering the non-linear coherent states of a quantum oscillator with variable mass, we propose a kernel function based on generalized hypergeometric functions, as orthogonal polynomial functions. The suggested kernel is implemented with support vector machine on two well known datasets (make_circles, and make_moons) and outperforms the baselines, even in the presence of high noise. In addition, we study impact of geometrical properties of feature space, obtaining by non-linear coherent states, on the SVM classification task, by using considering the Fubini-Study metric of associated coherent states.

I. INTRODUCTION

Quantum machine learning is a rapidly growing field of investigation. It can be argued that developments are being driven from two directions. Firstly, quantum computers offer the promise of massive improvement in the speed of computational processing [1–3]. Secondly, the mathematical framework of quantum mechanics is increasingly been seen as a suitable framework for designing algorithms that aren't constrained by Boolean algebra and logic [4, 5]. The reasons that support the latter claim are many, e.g., the linearity of the Schrödinger equation [6, 7], which leads to the definition of superposed states in complex Hilbert spaces with an interference term affecting probabilities. Consider modelling the dependence that measurement outcomes have on the preparation of states: duly named contextual scenarios [8]. There is also the novelty of correlations observed through entanglement, discord, *etc* in quantum mechanics that go beyond classically correlated structures [9, 10], as well as quasi-distributions, which occur in phase space, so-called Wigner distributions [11, 12], and achieve negativity - this is not possible in Kolmogorovian probability theory. All of the preceding introduce the potential for access to an information space greater than that of classical alternatives [13–16]. This is encouraging for scientists wishing to apply quantum formalism within machine learning (ML) as a generalisation of probability theory.

In ML, kernel methods [17–22] are a class of categorization algorithms. Used within a wide range of methods and algorithms, they include the support vector machine (SVM) [23–25], kernel operators with principal components analysis (PCA) [26], spectral cluster-

ing [27], canonical correlation analysis [28], linear adaptive filters [29], and ridge regression [30]. Indeed, kernel methods are proving to assist also in deep neural networks, for which there are many recently published works [31, 32]. There exist vast prospects of kernel methods in ML due to the non-linear nature of the underlying data. Within application settings, the data are usually non-separable, for which the requirement of the kernel then becomes transformations (of the data) into higher dimensions where it may be (linearly) separable as can be seen in Figure 1. One of the well-known kernel functions in ML, the Radial Basis function (RBF), is defined by $K(x, x') = \exp[-|x - x'|^2/2\sigma^2]$ where x and x' are two sample elements, and σ controls the decision boundary [33–35]. It is worthwhile to mention that the RBF can be understood as an inner product of the linear coherent state, see [36], which is defined as an eigenstate of the annihilation operator of a harmonic oscillator. The idea of using a quantum mechanics formalism in kernel methods was suggested by Schuld and Killoran, who introduced squeezed kernels in feature spaces [37]. In fact, they defined the feature space as a set of squeezed states so that the kernel is obtained by inner products of squeezed states [38, 39].

In this paper, we express non-linear coherent states [40–44] as a quantum feature space, such that kernel functions are defined as their inner products. We show that the mathematical structure of non-linear coherent states provides infinite kernels. As an example of non-linear feature space, we investigate coherent states constructed by wave-functions of a quantum oscillator with variable mass. Generalized hypergeometric functions, as orthogonal polynomials, are identified as provide the associated kernel. Our proposed KMNCS has been demonstrated in an SVM classifier, along with the RBF and squeezed kernel as a baseline on two-well-known datasets (make_moons, make_circles). KMNCS is shown to outperform the baselines (squeezed and RBF kernels) even as we increase the noise in the dataset (which increases difficulty of generalisation). In addition, we study the

*Electronic address: prayag.tiwari@dei.unipd.it

†Electronic address: shahram.dehdashti@qut.edu.au

‡Electronic address: p.bruza@qut.edu.au

§The first two authors contributed equally in this research.

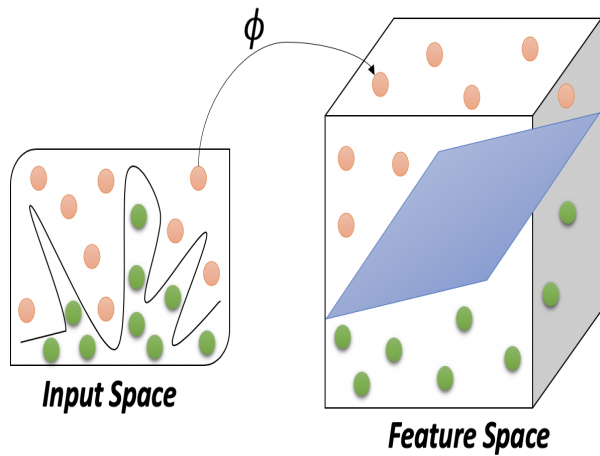


FIG. 1: Kernel visualization from low dimension input space to high dimension feature space.

geometrical properties of the feature space, by obtaining the Fubini-Study metric of non-linear coherent states. We show that the feature space of a non-linear coherent state of a oscillator with variable mass is a surface with negative curvature, which opens a new line of investigation of how the feature space's curvature affects the accuracy SVM classification.

The rest of the paper is organised as follows: in Section II, we briefly review the Kernel Method. Section III introduces the previously mentioned coherent states. Section IV provides an overview on non-linear coherent states and introduces the coherent states of a quantum oscillator with variable mass. This allows the main contribution of the paper to be defined: a kernel function based on generalized hypergeometric functions. Section V details the experimental design which allows the proposed kernel function to be empirically evaluated against two baseline: RBF and squeezed kernel. Section VI discusses the results of the empirical evaluation. Also, this section is examines the geometrical properties of a non-linear coherent state. Finally, Section VII concludes the article.

II. KERNEL METHOD

Traditional ML begins with a dataset of inputs $\mathcal{D} = \{x_1, \dots, x_M\}$ drawn from a set \mathcal{X} . The goal is to produce a predictive model that allows patterns to be discovered in yet to be observed data. Kernel methods use the inner product $K(x, x')$ between any given two inputs $x, x' \in \mathcal{X}$, as a distance measure to build predictive models that assist with representing characteristics of a data distribution.

Definition II.1. Let \mathcal{X} be a nonempty set, called the index set, and \mathcal{H} by a Hilbert space of functions $\phi: \mathcal{X} \rightarrow \mathbb{R}$. Then \mathcal{H} is called a reproducing kernel Hilbert space endowed with the dot product, $\langle \cdot | \cdot \rangle$, if there exists a func-

tion $k: \mathcal{X} \times \mathcal{X} \rightarrow \mathbb{R}$ with the two following properties: (i) k has the reproducing property, i.e., $\langle \phi | k(x, \cdot) \rangle = \phi(x)$ for all $\phi \in \mathcal{H}$; (ii) k spans \mathcal{H} [45].

Note that in particular $\langle k(x, \cdot) | k(x', \cdot) \rangle = k(x, x') = k(x', x)$ guarantees symmetry of the arguments of k .

Theorem II.1. Let $\phi: \mathcal{X} \rightarrow \mathcal{F}$ be a feature map. Kernel function can be defined as the inner product of two inputs mapped to some feature space by, $\mathbf{k}(x, x') = \langle \phi(x), \phi(x') \rangle$.

Proof. The proof can be found in references [20, 36]. \square

Theorem II.2. Consider a feature mapping is $\phi: \mathcal{X} \rightarrow \mathcal{F}$ over some input set \mathcal{X} , which provide the basis to a complex kernel $\mathbf{k}(x, x') = \langle \phi(x), \phi(x') \rangle$ that is defined on \mathcal{F} . The associated reproducing kernel Hilbert space can be written as $\mathcal{R}_{\mathbf{k}} = \{f: \mathcal{X} \rightarrow \mathbb{C}\}$

$$f(x) = \langle w, \phi(x') \rangle, \quad (1)$$

for all $w \in \mathcal{F}$ and $x \in \mathcal{X}$.

Proof. The proof can be found in [20] and [77]. \square

III. COHERENT STATE

A harmonic oscillator in quantum physics is described by the following Hamiltonian:

$$H = \hbar\omega \left(\hat{n} + \frac{1}{2} \right) \quad (2)$$

in which \hbar is the Planck's constant and ω is the angular frequency of the oscillator; the number operator \hat{n} is described by annihilation and creation operators, i.e., $\hat{n} = \hat{a}^\dagger \hat{a}$. The Schrödinger equation gives the discrete energy eigenvalue:

$$H |n\rangle = E_n |n\rangle, \quad n = 0, 1, 2, \dots \quad (3)$$

in which eigenvalue $E_n = \hbar\omega(n + 1/2)$ is associated by eigenstate $|n\rangle$. For simplicity, we consider $\hbar = 1$ and $\omega = 1$ in the rest of the paper.

A coherent state is the specific quantum state of the quantum harmonic oscillator, often described as a state which has dynamics most closely resembling the oscillatory behavior of a classical harmonic oscillator, for example see [46].

Definition III.1. A coherent state is defined as superposition of number state $|n\rangle$ as following:

$$|\alpha\rangle = e^{-|\alpha|^2/2} \sum_{n=0}^{\infty} \frac{\alpha^n}{\sqrt{n!}} |n\rangle \quad (4)$$

which number states satisfy $\langle n | m \rangle = \delta_{n,m}$, where $\delta_{n,m}$ is Kronecker delta.

Note that the inner product of two coherent states is given by:

$$\langle \alpha | \beta \rangle = e^{|\alpha - \beta|^2 / 2} \quad (5)$$

Lemma III.1. *A harmonic oscillator coherent state adheres the following:*

1. It is obtained by operation of the displacement operator $D(\alpha) = \exp\{\alpha^* a^\dagger - \alpha a\}$ on a reference state: $|\alpha\rangle = D(\alpha)|0\rangle$, in which $|\alpha\rangle$ is given by the relation (4).
2. It is an eigenvector of the annihilation operator, $a|\alpha\rangle = \alpha|\alpha\rangle$.
3. It fulfills the minimum uncertainty relation, i.e., $\Delta(\mathbf{x}) = \Delta(\mathbf{p}) = 1/\sqrt{2}$, where $\Delta(\mathbf{x}) = \sqrt{\langle \mathbf{x}^2 \rangle - \langle \mathbf{x} \rangle^2}$, where $\langle \mathbf{x} \rangle = \langle \alpha | \mathbf{x} | \alpha \rangle$.
4. It is over-complete, $K(\alpha, \alpha') = \langle \alpha | \alpha' \rangle \neq \delta(\alpha - \alpha')$, i.e., the equation (5), despite the fact that they fulfil the resolution of the identity, $\int d\mu(\mathbf{x}) |\mathbf{x}\rangle \langle \mathbf{x}| = \mathbb{I}$, which leads to the following relation:

$$\int d\mu(\mathbf{x}) \langle \phi | \mathbf{x} \rangle \langle \mathbf{x} | \psi \rangle = \langle \phi | \psi \rangle. \quad (6)$$

Proof. The proofs can be found in references [36, 46]. \square

The latter, i.e., item 4 of Lemma III.1, implies an arbitrary function can be expressible as a linear combination of kernel functions in a ‘‘reproducing Hilbert space’’ [47]. We should mention that the first above-mentioned property leads to define a displacement-type coherent states [46], for generalized annihilation and creation operators. Moreover a Gazeau-Klauder coherent state is defined by the second property and fulfils the third property [46]. It should be noted that while the latter, i.e., resolution of the identity, fulfils all types of coherent states.

Recently Schuld and Killoran published a paper in which data is mapped into a feature space established by squeezed states [37]. Squeezed states are states that saturate the Heisenberg uncertainty principle; additionally, the quadrature variance of position and momentum depend on a parameter, so-called squeezing parameter. The squeezing parameter causes the uncertainty to be squeezed one of its quadrature components, while stretched uncertainty for the other component, i.e. $\Delta(\mathbf{x}) = \exp\{2\zeta\}/\sqrt{2}$ and $\Delta(\mathbf{p}) = \exp\{-2\zeta\}/\sqrt{2}$, where ζ is the squeezing parameter. Therefore, the squeezing parameter controls uncertainty via a quadrature component, while the third and fourth properties of coherent states are preserved. However, as we mentioned, one of the well-known kernel functions in ML, the Radial Basis function (RBF), is defined by

$$K(\mathbf{x}, \mathbf{x}'; \sigma) = \exp\{-\|\mathbf{x} - \mathbf{x}'\|^2 / 2\sigma^2\}, \quad (7)$$

where \mathbf{x} and \mathbf{x}' are two sample elements, and σ is understood as a free parameter. However, drawing a comparison between relations (5) and (7), inspires someone to

interpret the RBF as an inner product of two coherent states. This interpretation opens the door to define new kernels and consequently improve the kernel method [36].

IV. NON-LINEAR COHERENT STATE

As mentioned before, some efforts have been devoted to study possible generalization of the quantum harmonic oscillator algebra [41]. A deformed algebra is a non-trivial generalization of a given algebra through the introduction of one or more deformation parameters, such that, in a certain limit of the parameters, the non-deformed algebra can be recovered.

A particular deformation of the W-H algebra led to the notion of f -deformed oscillator [41]. An f -deformed oscillator is a non-harmonic system where its dynamical variables (creation and annihilation operators) are constructed from a non-canonical transformation through

$$\hat{A} = \hat{a}f(\hat{n}) = f(\hat{n} + 1)\hat{a}, \quad (8)$$

$$\hat{A}^\dagger = f^\dagger(\hat{n})\hat{a}^\dagger = \hat{a}^\dagger f^\dagger(\hat{n} + 1). \quad (9)$$

where $f(\hat{n})$ is called deformation function by which non-linear properties of this system are governed. An f -deformed oscillator is characterized by a Hamiltonian of the harmonic oscillator form,

$$\hat{H} = \frac{\omega}{2} (\hat{A}\hat{A}^\dagger + \hat{A}^\dagger\hat{A}), \quad (10)$$

where \hat{A} and \hat{A}^\dagger are given in equations (8) and (9). In this Hamiltonian, ω is frequency of harmonic oscillator and $\hbar = m = 1$. The deformed operators satisfy the following commutation relation

$$[\hat{A}, \hat{A}^\dagger] = (\hat{n} + 1)f^2(\hat{n} + 1) - \hat{n}f^2(\hat{n}). \quad (11)$$

Relations (8) and (9) give eigenvalues of the Hamiltonian (10) as follows:

$$E_n = \frac{\omega}{2} ((n + 1)f^2(n + 1) + nf^2(n)). \quad (12)$$

It is worth to mention that by approaching deformation function into 1, i.e., $f(n) \rightarrow 1$, the non-deformation energy eigenvalues, $E_n = \omega(n + \frac{1}{2})$, and the non-deformed commutation relation $[\hat{a}, \hat{a}^\dagger] = 1$ are recovered. However, similar to the harmonic oscillator, it is possible to construct coherent states for the f -deformed oscillator. The non-linear transformation of the creation and annihilation operators leads naturally to the notion of non-linear coherent states or f -coherent states [48–51].

Definition IV.1. *Non-linear coherent states are defined as the right-hand eigenstates of the deformed annihilation operator \hat{A} as follows [46]:*

$$\hat{A}|\alpha\rangle_f = \alpha|\alpha\rangle_f. \quad (13)$$

From equation (13) one can obtain an explicit form of the non-linear coherent states in the number state representation as,

$$|\alpha\rangle_f = \frac{1}{\mathcal{N}} \sum_n^M \frac{\alpha^n}{\sqrt{n![f(n)]!}} |n\rangle, \quad (14)$$

where M can be finite, or infinite (corresponding to finite or infinite dimensional Hilbert space), α is a complex number and $[f(n)]! = \prod_{i=0}^n f(i)$, with $[f(0)]! = 1$; the normalization factor \mathcal{N} is given by

$$\mathcal{N} = \left(\sum_{n=0}^M \frac{|\alpha|^{2n}}{n![f(n)]!} \right)^{-1/2}. \quad (15)$$

Therefore, based on the definition II.1, we can define a kernel as the following:

Definition IV.2. By mapping multi-dimensional input set $\mathbf{x} = (x_1, \dots, x_N)^T \in \mathbb{R}^N$ into non-linear coherent states, defined by the relation (14), so that they are fulfilled with resolution of the identity, a feature space is defined as

$$\phi : (x_1, \dots, x_N) \rightarrow |x_1\rangle_f \otimes |x_2\rangle_f \otimes \dots \otimes |x_N\rangle_f.$$

In addition, the associated kernel is obtained by the inner product as the following:

$$K(\mathbf{x}, \mathbf{x}') = \prod_{i=1}^N {}_f\langle x_i | x'_i \rangle_f, \quad (16)$$

in which

$${}_f\langle x_i | x'_i \rangle_f = \frac{1}{\mathcal{N}^2} \sum_{n=0}^M \frac{(x_i x'_i)^n}{m![f(m)]!}. \quad (17)$$

A. Non-Linear coherent state of an oscillator with variable mass

The quantum version of a non-linear oscillator Hamiltonian with variable mass is given by [52]

$$H = \frac{1}{2\lambda} \left[-(1 + \delta^2 x^2) \frac{d^2}{dx^2} - 2\delta^2 x \frac{d}{dx} + \frac{\lambda^2 x^2}{1 + \delta^2 x^2} \right] \quad (18)$$

in which where λ is a real parameter and δ is constant that measures the force of the nonlinearity of the oscillator. By using ladder operators, one can define a non-linear coherent state as the following:

$$|x\rangle = \frac{1}{\mathcal{N}(x)} \sum_{n=0}^{\infty} \frac{x^n}{\rho_n} |n\rangle \quad (19)$$

in which $\rho_n = n!(-k)^n(2 - 1/k)_n$, which $(u)_n = u(u-1) \dots (u+n-1)$ represents the Pochhammer symbol, $k =$

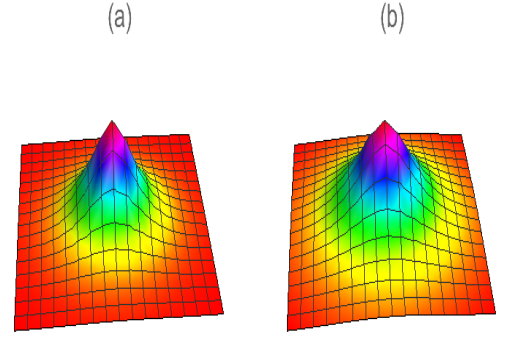


FIG. 2: Schematic shape of the kernel function (22) for $k = -0.001$ and $k = -0.5$ in plots (a) and (b), respectively. The input x is fixed at $(0, 0)$ and x' is varied.

$\delta^2/2\lambda$ and normalization factor $\mathcal{N}(x)$ is given by

$$\begin{aligned} \mathcal{N}^2(x) &= \sum_{n=0}^{\infty} \left(\frac{(1/k)^n}{n!(2 - 1/k)_n} \right)^2 |x|^{2n} \\ &= {}_0F_3(; 1, 2 - 1/k, 2 - 1/k; |x/k|^2) \end{aligned} \quad (20)$$

which ${}_0F_3(; 1, 2 - 1/k, 2 - 1/k; |x/k|^2)$ is a generalized hyper-geometric function.

By considering a multi-dimensional input set in a data set of vectors $\mathbf{x} = (x_1, \dots, x_N)^T \in \mathbb{R}^N$, one can define the joint state of N deformed coherent states,

$$\phi : (x_1, \dots, x_N) \rightarrow |x_1, k\rangle \otimes |x_2, k\rangle \otimes \dots \otimes |x_N, k\rangle.$$

Therefore, the kernel is defined as the following:

$$K(\mathbf{x}, \mathbf{x}') = \prod_{i=1}^N \langle x_i; k | x'_i; k \rangle, \quad (21)$$

in which

$$\langle x_i; k | x'_i; k \rangle = \frac{{}_0F_3(; 1, 2 - 1/k, 2 - 1/k; x_i x'_i / k^2)}{\mathcal{N}(x) \mathcal{N}(x')} \quad (22)$$

Figure 2 schematically illustrates the kernel function (22), for $k = -0.001$ and $k = -0.05$.

B. Geometrical properties of associated Hilbert Space constructed by Non-linear coherent state

For understanding the rule of nonlinear parameter k , we will study the geometrical properties of above-mentioned feature spaces. We can define the line element of the feature space by using the Fubini-Study metric [53].

Definition IV.3. A suitable metric between two Hilbert space vectors, e.g. $|\psi\rangle$ and $|\phi\rangle$, is defined by

$$d(|\psi\rangle, |\phi\rangle) = \min || |\psi\rangle - e^{i\alpha} |\phi\rangle ||, \quad 0 \leq \alpha \leq 2\pi. \quad (23)$$

The infinitesimal form of this metric is given by the Fubini-Study metric:

$$ds^2 = ||d|x\rangle||^2 - ||\langle x | d|x\rangle||^2. \quad (24)$$

The following gives the Fubini-Study metric of a non-linear coherent state (19).

Theorem IV.1. *The Fubini-Study metric of a non-linear coherent state (19) is a surface with non-zero curvature with the following metric:*

$$ds^2 = \Omega(r) (dr^2 + r^2 d\phi^2), \quad (25)$$

in which

$$\Omega(r) = \frac{1}{2} \left[\frac{\partial_r^2 \mathcal{N}(r)}{\mathcal{N}(r)} + \frac{\partial_r \mathcal{N}(r)}{r \mathcal{N}(r)} - \left(\frac{\partial_r \mathcal{N}(r)}{\mathcal{N}(r)} \right)^2 \right]. \quad (26)$$

with $\partial_r \equiv \frac{\partial}{\partial r}$.

Proof. We consider the $x = r e^{i\phi}$, using the definition (24), directly leads to the metric (25).

By using the definition of Christoffel symbol,

$$\Gamma_{ab}^c = \frac{1}{2} g^{cd} (\partial_a g_{bd} + \partial_b g_{ad} - \partial_d g_{ab}), \quad a, b, c = r, \phi \quad (27)$$

with the Einstein summation rule, the non-zero Christoffel symbols are given by

$$\Gamma_{rr}^r = \frac{1}{2} \partial_r \ln \Omega(r), \quad (28)$$

$$\Gamma_{\phi\phi}^r = - \left(r + \frac{r^2}{2} \partial_r \ln \Omega(r) \right), \quad (29)$$

$$\Gamma_{\phi r}^\phi = \frac{1}{r} + \frac{1}{2} \partial_r \ln \Omega(r). \quad (30)$$

Hence, the non-zero Ricci tensors are given by,

$$R_{rr} = -\frac{1}{2} \left(\partial_r^2 \ln \Omega(r) + \frac{1}{r} \partial_r \ln \Omega(r) \right) \quad (31)$$

$$R_{\phi\phi} = -\frac{r}{2} (\partial_r \ln \Omega(r) + r \partial_r^2 \ln \Omega(r)) \quad (32)$$

Hence, the Ricci scalar, $R = g^{ab} R_{ab}$, is obtained as

$$R = -\Omega(r)^{-1} \left(\partial_r^2 \ln \Omega(r) + \frac{1}{r} \partial_r \ln \Omega(r) \right) \quad (33)$$

□

It is worthwhile to note that the metric (25), which describes the feature space, is a surface that is conformal with flat space, that is conformally preserves angles, while lengths can be changed. In fact, this metric illustrates a two-dimensional curved space, depending on conformal function $\Omega(r)$. By considering the non-linear coherent state (19) and normalized coefficient (5), Fig. 3 represents the Ricci scalar for different values of k . This figure indicates that the feature space is a surface with negative curvature. Decreasing the value k causes the Ricci curvature to increase. In other words, increasing value of k causes the feature space and the associated kernel to approach a flat space and RBF kernel, respectively. Despite the fact that the feature space constructed on a non-linear coherent state is a non-zero curved space, RBF, which is constructed from a linear coherent state, is a kernel on flat space, with the zero Ricci scalar.

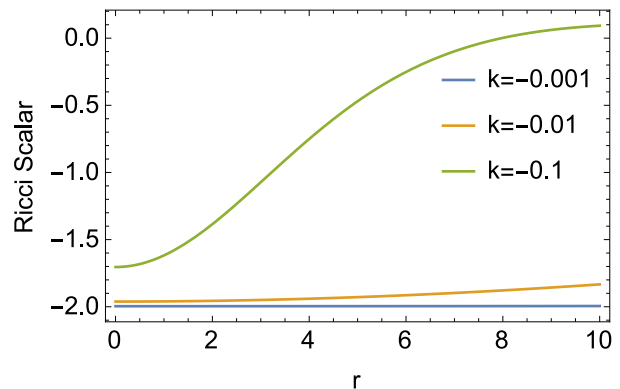


FIG. 3: Ricci scalar of the Fubini-Study metric of a feature space constructed by a oscillator with variable mass as function of r , for different values of k .

V. EXPERIMENTAL DESIGN

In the following, we empirically evaluate the KMNCS, i.e. the relation (21), RBF kernel, i.e., the relation (7), and the Squeezed kernel, given by

$$K_{Sq} = \prod_{i=1} \left[\frac{\text{sech } c \text{ sech } c'}{1 - e^{i(x-x')} \tanh c \tanh c'} \right]^{1/2}. \quad (34)$$

SVM uses a kernel function to define a decision boundary for separating the data points. Generally, the hyperparameter C in the Gaussian kernel is used to optimize the performance of SVM, as a cost function connected with mis-classifications of data points in feature space of the training set. We kept the hyperparameter $C = 1$ as the optimal value.

In order to provide a comprehensive picture of the performance of the kernels, i.e., kernels (7), (34) and (21), noise was systematically applied to the input data. Applying noise implies adding it to the target variable. For example, if the noise parameter is say 0.2, a standard deviation of 0.2 would be observed (originating from Gaussian noise) in the output. When data points become inseparable due to noise, it becomes more challenging for the classifier to accurately classify the data points.

We have used synthetic datasets (simple toy datasets) which are commonly used to check the performance of kernels. The two datasets (*make_moons*[78] and *make_circles*[79]) are taken from sklearn. There is some flexibility in regard to each dataset. Random noise can be introduced by adjusting different parameters for each dataset: the **Moons** dataset generates two half circles with the noise parameters affecting 'interleave', the **Circles** dataset generates concentric circles also affected by 'interleave' via the noise parameter. The decision region for class 1 is color-coded 'red', and 'blue' for class 0. We have also recorded differing values of *flip-y* which is an inbuilt parameter in *make_classification* [80] (Generate a random n-class classification problem) also from sklearn. A large *flip-y* supplements the noise ef-

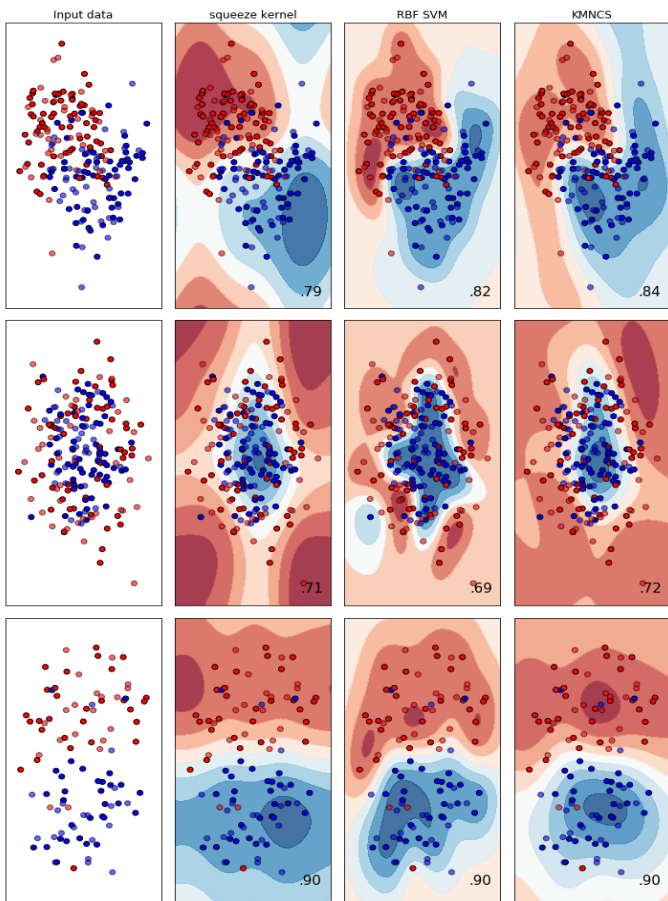


FIG. 4: Kernel visualization (Squeezed, RBF kernels and KMNCs) for $k = -0.001$, while the noise is 0.4 on both the `make_moons` and `make_circles` datasets.

fects, making accurate classification even more challenging. The `factor` and `random_state` in the setting have also been recorded. We have divided the data into 60% training set and 40% test set. We have also used 5 fold cross validation during training in order to avoid overfitting problems. We have examined KMNCs using different values of k in order to evaluate the classification performance and to understand how the decision boundaries are formed.

VI. RESULTS

The `sklearn` package includes a “fit” method that is used for informing the model by applying a training set. To compute the score by cross-validation of SVM, “`cross_val_score`” is used also from `sklearn` with a “5”-fold cross-validation.

As we can see from Table I, KMNCs has been tested on several values of k . If we check the value of $k = -0.001$ with very low noise, i.e. = 0.1, all the three kernels provide almost the same classification accuracy as can be seen in Figure 6 (Here the input data is separable and it is

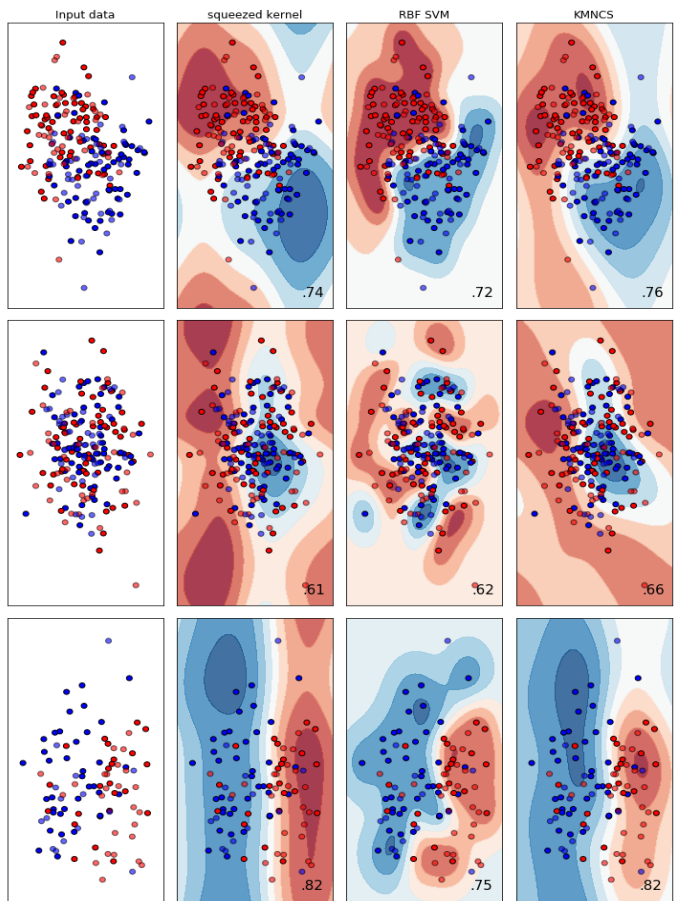


FIG. 5: Kernel visualization (Squeezed, RBF, and KMNCs) for $k = -0.1$, while noise is 0.5 on the `make_moons` dataset, and 0.7 on the `make_circles` dataset.

an easy task for the classifier to classify them). Interestingly, KMNCs has better performance than both baselines for both datasets when $k = -0.001$ and noise is 0.4. This performance in the presence of such noise demonstrates effectiveness of KMNCs. The decision boundary is depicted in Figure 4.

When we increase the noise effect in the data, then classification becomes more challenging i.e., when noise is 0.5 then KMNCs outperforms the squeezed and RBF kernel as can be seen in Figure 5. Note that it is possible to increase the accuracy of the classifier if we select $k = -0.01, -0.1$ with the same level of noise, that is 0.5, as it can be seen in the Table I. The KMNCs performance is deemed better than the baselines as data is inseparable (due to 50% noise in the target variable). Again, where noise is 0.7 and $k = -0.1$, then KMNCs provides better performance than the two baseline classifiers due to clean decision boundaries where data is separable, as can be seen in Figure 5.

We also tested on 3000 samples as can be seen in Table III. KMNCs outperforms both baselines which suggests it is effective on larger samples by producing clean decision boundaries.

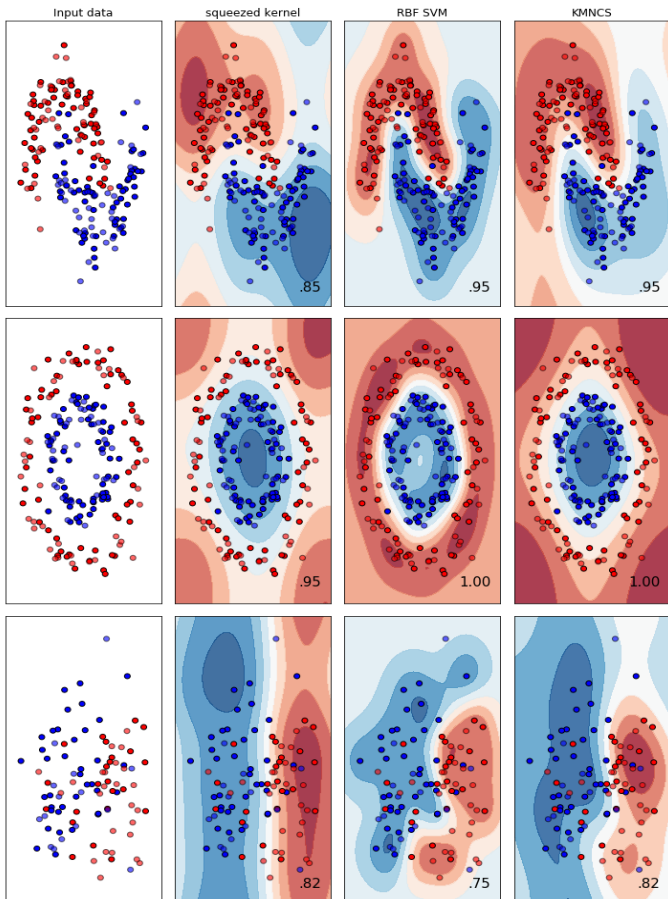


FIG. 6: Kernel visualization (Squeezed, RBF, and KMNCS) for $k = -0.01$, while noise is 0.2 on the make_moons dataset, and 0.1 on make_circles dataset.

There is a trade-off with decision boundaries and accuracy. It is possible to achieve even higher accuracy if we continue to modify k , however this may obscure the decision boundaries (despite high accuracy scores), which could be related to bias and variance issues. We also computed the score without the cross validation set with the results presented in Table II.

VII. DISCUSSION

With respect to the general behaviour of KMNCS, it can be said that the kernel is conducive to forming large decision boundaries, which is a major point of contrast when considering the RBF kernel, as evident in Figure 4.5. As previously mentioned, the hyper-parameter C can be used to optimise an SVM classifier, as a cost function associated with mis-classification of elements in feature spaces of the training set. It implies the maximisation of C tightens decision boundaries (so called hard margins), and was introduced by Boser *et al.* [54]. In later work, 'hard' margins were found to fail on even slightly inseparable data. As a solution, [55] introduced a

TABLE I: Accuracy on Squeezed kernel, RBF, and **KMNCS** on the make_moons and make_circles datasets with the following parameters: n_samples=200, random_state=50, y_flip=0.2, factor=0.5, n_informative=2, 5-fold cross validation. Noise effects are introduced in the data to increase difficulty of accurate classification.

Parameters		moons	circles
Squeezed Kernel	Noise=0.1	0.90	0.95
	Noise=0.2	0.85	0.86
	Noise=0.3	0.82	0.80
	Noise=0.4	0.79	0.71
	Noise=0.5	0.74	0.68
	Noise=0.7	0.62	0.61
RBF	Noise=0.1	0.99	1.0
	Noise=0.2	0.95	0.90
	Noise=0.3	0.89	0.80
	Noise=0.4	0.82	0.69
	Noise=0.5	0.72	0.64
	Noise=0.7	0.65	0.62
KMNCS	Noise=0.1, k=-0.001	0.97	1.0
	Noise=0.2, k=-0.001	0.95	0.88
	Noise=0.2, k=-0.01	0.95	0.89
	Noise=0.2, k=-0.1	0.94	0.88
	Noise=0.3, k=-0.001	0.90	0.79
	Noise=0.3, k=-0.01	0.90	0.79
	Noise=0.4, k=-0.001	0.84	0.72
	Noise=0.4, k=-0.01	0.84	0.72
	Noise=0.5, k=-0.001	0.75	0.68
	Noise=0.5, k=-0.01	0.76	0.69
	Noise=0.5, k=-0.1	0.76	0.70
	Noise=0.7, k=-0.001	0.64	0.62
Noise=0.7, k=-0.01	0.62	0.62	
Noise=0.7, k=-0.1	0.65	0.66	

TABLE II: Accuracy on same parameters from Table I without cross validation

Parameters		moons	circles
Squeezed Kernel	Noise=0.2	0.90	0.94
	Noise=0.5	0.75	0.70
	Noise=0.7	0.68	0.56
RBF	Noise=0.2	0.96	0.90
	Noise=0.5	0.76	0.64
	Noise=0.7	0.70	0.54
KMNCS	Noise=0.2, k=-0.001	0.99	0.93
	Noise=0.5, k=-0.001	0.75	0.66
	Noise=0.7, k=-0.001	0.71	0.54

meaningful technique for the minimisation of C that was found to enlarge the space covered by decision boundaries ('soft' margins). While this has largely benefited the field of SVM in contention with other classification techniques, the trade-off is that significantly 'soft' margins fail to classify data entirely - formally known as over-generalisation, large decision boundaries (as produced by the Squeezed kernel) become non-representative of the data. As a result, the objective is to minimise the hyper-parameter C , while maintaining the highest possible classification. Relating this back to the findings of this paper, the topological structure of the KMNCS is reminiscent of

TABLE III: Accuracy on 3000 samples with same parameters from Table I as well as 5-fold cross validation

	Parameters	moons	circles
Squeezed Kernel	Noise=0.5	0.81	0.65
	Noise=0.8	0.72	0.55
	Noise=1.0	0.68	0.52
RBF	Noise=0.5	0.81	0.64
	Noise=0.8	0.73	0.54
	Noise=1.0	0.68	0.51
KMNCS	Noise=0.5, k=-0.1	0.82	0.65
	Noise=0.5, k=-0.01	0.81	0.65
	Noise=0.8, k=-0.1	0.73	0.56
	Noise=1.0, k=-0.1	0.69	0.53

Ref. [54], surprisingly in cases of sparse data (in this case the sparse *make_moons* dataset), without concern for C .

VIII. CONCLUSIONS AND REMARKS

In this paper, we mapped datasets into non-linear coherent states, as a non-linear feature space, constructed by a complex Hilbert space. We showed that the RBF kernel is recovered when data is mapped to a complex Hilbert space represented by coherent states. Therefore, non-linear coherent states can be considered as natural generalized candidates for formalizing kernels. In addition, by considering the non-linear coherent states of a quantum oscillator with variable mass, we proposed a kernel function based on generalized hypergeometric functions. This idea suggests a method for obtaining a generalized kernel function which can be expressed by

orthogonal polynomial functions on the one hand, and opens a new door for using quantum formalism to specify quantum algorithms in continuous variable quantum computing, on the other. In addition, we studied the geometrical properties of the surface in which the kernel lives. We indicated that the feature space of a non-linear coherent state is a non-zero curved space, despite the fact that the RBF kernel lives on feature space which is flat. This method can potentially open a door for studying the impact of general curved space on the machine learning methods more generally, and the problem of classification more specifically.

More generally, this research has demonstrated how quantum approaches to machine learning may prove beneficial. In practical usage, machine learning applications of quantum theory have begun involving developments of physical circuitry [56]. These contributions have begun to realise the quantum processing components required to build quantum computational devices designed solely for feature classification. It is inspiring to think that eventually, SVM classification may (with the assistance of quantum theory) be computed substantially faster than ever before.

Acknowledgments

This reserach has received funding from the European Union’s Horizon 2020 research and innovation programme under the Marie Skłodowska-Curie grant agreement No 721321. It was additionally supported by the Asian Office of Aerospace Research and Development (AOARD) grant: FA2386-17-1-4016.

-
- [1] S. Aaronson and A. Arkhipov, arXiv preprint arXiv:1309.7460 (2013).
- [2] M. Tillmann, B. Dakić, R. Heilmann, S. Nolte, A. Szameit, and P. Walther, *Nature photonics* **7**, 540 (2013).
- [3] D. J. Brod, E. F. Galvão, A. Crespi, R. Osellame, N. Spagnolo, and F. Sciarrino, *Advanced Photonics* **1**, 034001 (2019).
- [4] I. Pitowsky, *The British Journal for the Philosophy of Science* **45**, 95 (1994).
- [5] A. Vourdas, *Journal of Physics A: Mathematical and Theoretical* (2019).
- [6] E. Schrödinger, *Schrödinger: Centenary celebration of a polymath* (CUP Archive, 1987).
- [7] Y. Tsutsumi, *Funkcialaj Ekvacioj* **30**, 115 (1987).
- [8] S. Kochen and E. P. Specker, in *The logico-algebraic approach to quantum mechanics* (Springer, 1975), pp. 293–328.
- [9] W. H. Zurek, *Annalen der Physik* **9**, 855 (2000).
- [10] D. Girolami, A. M. Souza, V. Giovannetti, T. Tufarelli, J. G. Filgueiras, R. S. Sarthour, D. O. Soares-Pinto, I. S. Oliveira, and G. Adesso, *Physical Review Letters* **112**, 210401 (2014).
- [11] R. Simon, E. Sudarshan, and N. Mukunda, *Physical Review A* **36**, 3868 (1987).
- [12] C. Lorce and B. Pasquini, *Physical Review D* **84**, 014015 (2011).
- [13] K. T. Goh, J. Kaniewski, E. Wolfe, T. Vértesi, X. Wu, Y. Cai, Y.-C. Liang, and V. Scarani, *Physical Review A* **97**, 022104 (2018).
- [14] M. F. Pusey, L. Del Rio, and B. Meyer, arXiv preprint arXiv:1904.08699 (2019).
- [15] S. Dehdashti, L. Fell, and P. Bruza, *Entropy* **22**, 174 (2020).
- [16] S. Uprety, P. Tiwari, S. Dehdashti, L. Fell, D. Song, P. Bruza, and M. Melucci, *Advances in Information Retrieval* **12035**, 728 (2020).
- [17] J. Shawe-Taylor, N. Cristianini, et al., *Kernel methods for pattern analysis* (Cambridge university press, 2004).
- [18] D. Zelenko, C. Aone, and A. Richardella, *Journal of machine learning research* **3**, 1083 (2003).
- [19] R. Soentpiet, *Advances in kernel methods: support vector learning* (MIT press, 1999).
- [20] T. Hofmann, B. Schölkopf, and A. J. Smola, *The annals of statistics* pp. 1171–1220 (2008).
- [21] T. Evgeniou, C. A. Micchelli, and M. Pontil, *Journal of Machine Learning Research* **6**, 615 (2005).
- [22] C. Campbell, *Neurocomputing* **48**, 63 (2002).
- [23] S.-i. Amari and S. Wu, *Neural Networks* **12**, 783 (1999).

- [24] L. Wang, *Support vector machines: theory and applications*, vol. 177 (Springer Science & Business Media, 2005).
- [25] W. S. Noble, *Nature biotechnology* **24**, 1565 (2006).
- [26] B. Schölkopf, A. Smola, and K.-R. Müller, in *International conference on artificial neural networks* (Springer, 1997), pp. 583–588.
- [27] I. S. Dhillon, Y. Guan, and B. Kulis, in *Proceedings of the tenth ACM SIGKDD international conference on Knowledge discovery and data mining* (ACM, 2004), pp. 551–556.
- [28] S. Akaho, arXiv preprint cs/0609071 (2006).
- [29] W. Liu, I. Park, and J. C. Principe, *IEEE transactions on neural networks* **20**, 1950 (2009).
- [30] S. An, W. Liu, and S. Venkatesh, in *2007 IEEE Conference on Computer Vision and Pattern Recognition* (IEEE, 2007), pp. 1–7.
- [31] Y. Cho and L. K. Saul, in *Advances in neural information processing systems* (2009), pp. 342–350.
- [32] M. Belkin, S. Ma, and S. Mandal, arXiv preprint arXiv:1802.01396 (2018).
- [33] M. T. Musavi, W. Ahmed, K. H. Chan, K. B. Faris, and D. M. Hummels, *Neural networks* **5**, 595 (1992).
- [34] M. D. Buhmann, *Acta numerica* **9**, 1 (2000).
- [35] M. J. Orr et al., *Introduction to radial basis function networks* (1996).
- [36] J. M. Kübler, K. Muandet, and B. Schölkopf, *Physical Review Research* **1**, 033159 (2019).
- [37] M. Schuld and N. Killoran, *Physical review letters* **122**, 040504 (2019).
- [38] R. Datko, *Journal of Mathematical analysis and applications* **32**, 610 (1970).
- [39] A. M. Gleason, *Journal of mathematics and mechanics* pp. 885–893 (1957).
- [40] R. de Matos Filho and W. Vogel, *Physical Review A* **54**, 4560 (1996).
- [41] V. Man’ko, G. Marmo, E. Sudarshan, and F. Zaccaria, *Physica Scripta* **55**, 528 (1997).
- [42] S. Mancini, *Physics Letters A* **233**, 291 (1997).
- [43] B. Roy and P. Roy, *Journal of Optics B: Quantum and Semiclassical Optics* **2**, 65 (2000).
- [44] S. Sivakumar, *Journal of Optics B: Quantum and Semiclassical Optics* **2**, R61 (2000).
- [45] B. Scholkopf and A. J. Smola, *Learning with kernels: support vector machines, regularization, optimization, and beyond* (MIT press, 2001).
- [46] S. T. Ali, J.-P. Antoine, J.-P. Gazeau, et al., *Coherent states, wavelets and their generalizations*, vol. 3 (Springer, 2000).
- [47] M. Combescure and D. Robert, *Coherent states and applications in mathematical physics* (Springer Science & Business Media, 2012).
- [48] S. Dehdashti, M. B. Harouni, B. Mirza, and H. Chen, *Physical Review A* **91**, 022116 (2015).
- [49] S. Dehdashti, A. Mahdifar, M. B. Harouni, and R. Roknizadeh, *Annals of Physics* **334**, 321 (2013).
- [50] S. Dehdashti, A. Mahdifar, and R. Roknizadeh, *International Journal of Geometric Methods in Modern Physics* **10**, 1350014 (2013).
- [51] S. Dehdashti, R. Li, J. Liu, F. Yu, and H. Chen, *AIP Advances* **5**, 067165 (2015).
- [52] M. Tchoffo, F. Migueu, M. Vubangsi, and L. Fai, *Heliyon* **5**, e02395 (2019).
- [53] I. Bengtsson and K. Życzkowski, *Geometry of quantum states: an introduction to quantum entanglement* (Cambridge university press, 2017).
- [54] B. E. Boser, I. M. Guyon, and V. N. Vapnik, in *Proceedings of the fifth annual workshop on Computational learning theory* (ACM, 1992), pp. 144–152.
- [55] P. Schilkopf, C. Burgest, and V. Vapnik, in *Proceedings of the 1st international conference on knowledge discovery & data mining* (1995), pp. 252–257.
- [56] V. Havlíček, A. D. Córcoles, K. Temme, A. W. Harrow, A. Kandala, J. M. Chow, and J. M. Gambetta, *Nature* **567**, 209 (2019).
- [57] A. J. Smola, S. Vishwanathan, and T. Hofmann, in *AIS-TATS* (Citeseer, 2005).
- [58] J. Zhuang, I. W. Tsang, and S. C. Hoi, in *Proceedings of the Fourteenth International Conference on Artificial Intelligence and Statistics* (2011), pp. 909–917.
- [59] M. Planck, *Nobel lecture* **2**, 1 (1920).
- [60] A. K. Ekert, *Physical review letters* **67**, 661 (1991).
- [61] A. Steane, *Reports on Progress in Physics* **61**, 117 (1998).
- [62] E. O. Kiktenko, N. O. Pozhar, M. N. Anufriev, A. S. Trushechkin, R. R. Yunusov, Y. V. Kurochkin, A. Lvovsky, and A. Fedorov, *Quantum Science and Technology* **3**, 035004 (2018).
- [63] L. Mandel and E. Wolf, *Optical coherence and quantum optics* (Cambridge university press, 1995).
- [64] M. Harouni, Z. Harsij, J. Shen, H. Wang, Z. Xu, B. Mirza, and H. Chen, *Quantum Information & Computation* **16**, 1365 (2016).
- [65] E. P. Wigner, in *Part I: Physical Chemistry. Part II: Solid State Physics* (Springer, 1997), pp. 110–120.
- [66] C. K. Zachos, D. B. Fairlie, and T. L. Curtright, *Quantum mechanics in phase space: an overview with selected papers* (World Scientific, 2005).
- [67] Y.-C. Liang, R. W. Spekkens, and H. M. Wiseman, *Physics Reports* **506**, 1 (2011).
- [68] R. Rosipal and L. J. Trejo, *Journal of machine learning research* **2**, 97 (2001).
- [69] A. W. Harrow, A. Hassidim, and S. Lloyd, *Physical review letters* **103**, 150502 (2009).
- [70] O. Chapelle, B. Scholkopf, and A. Zien, *IEEE Transactions on Neural Networks* **20**, 542 (2009).
- [71] P. Rebentrost, M. Mohseni, and S. Lloyd, *Physical review letters* **113**, 130503 (2014).
- [72] S. Aaronson, *Nature Physics* **11**, 291 (2015).
- [73] J. J. Sakurai and E. D. Commins, *Modern quantum mechanics, revised edition* (1995).
- [74] S. K. Zhou and R. Chellappa, *IEEE transactions on pattern analysis and machine intelligence* **28**, 917 (2006).
- [75] G. Wahba, *Proceedings of the National Academy of Sciences* **99**, 16524 (2002).
- [76] S. Dehdashti, C. Moreira, A. K. Obeid, and P. Bruza, arXiv preprint arXiv:2006.02904 (2020).
- [77] http://www.gatsby.ucl.ac.uk/~protect/protect/unhbox\voidb@x\penalty\@M\{}gretton/coursefiles/lecture4_introToRKHS.pdf
- [78] https://scikit-learn.org/stable/modules/generated/sklearn.datasets.make_moons.html#sklearn.datasets.make_moons
- [79] https://scikit-learn.org/stable/modules/generated/sklearn.datasets.make_circles.html#sklearn.datasets.make_circles
- [80] https://scikit-learn.org/stable/modules/generated/sklearn.datasets.make_classification

```
html#sklearn.datasets.make_classification
```